Role of Retained Austenite in Medium Manganese Steels

A progress report submitted
in partial fulfilment of the CP302 project

by

Paidi Satwika
(2022MMB1387)

Under the Guidance of
Dr. Avala Lava Kumar

DEPARTMENT OF METALLURGICAL AND
MATERIALS ENGINEERING

INDIAN INSTITUTE OF TECHNOLOGY ROPAR

May 2025

Executive Summary

Background: Medium manganese steels are promising materials for automotive applications due to their excellent combination of strength and ductility. This is largely due to retained austenite, a phase that transforms under stress, enhancing mechanical performance through TRIP and TWIP effects. However, detecting and stabilizing retained austenite is challenging due to its fine dispersion and low volume fraction.

Problem Statement: Retained austenite significantly improves mechanical properties, but its instability and low detectability limit its effectiveness in medium Mn steels.

Hypothesis: We hypothesize that optimizing alloy composition and heat treatment can stabilize retained austenite, enhancing both strength and ductility through TRIP/TWIP mechanisms.

Conceptual Approach:

- Characterize microstructure using optical microscopy and XRD
- Identify phase composition with SEM-EDX
- Measure phase-specific mechanical properties via nanoindentation
- Correlate retained austenite with mechanical behavior
- Suggest processing improvements to retain more austenite

Preliminary Work: Initial tests confirm a ferrite-dominated microstructure with small amounts of austenite and martensite. Mechanical differences among phases have been observed using nanoindentation.

Deliverables:

- Phase identification and fraction analysis
- Mechanical property mapping
- Recommendations to stabilize retained austenite
- Final report with findings and proposed improvements

Impact: This study supports the development of stronger, more ductile steels, contributing to safer and lighter automotive components and advancing high-performance structural materials.

Table of Contents

List of Figures

List of Tables

CHAPTER 1

Introduction

In today's pursuit of safer, lighter, and more energy-efficient vehicles, the demand for advanced materials with exceptional mechanical performance has increased rapidly. Traditional steels often fall short in providing the ideal balance between strength and ductility required in automotive and structural components. Medium manganese (Mn) steels have emerged as promising candidates in this context, offering high strength along with excellent formability and energy absorption. These steels enable significant weight reduction in vehicles without compromising crash safety—making them highly relevant for next-generation automotive and structural applications. Their unique microstructural features allow activation of advanced deformation mechanisms such as TRIP (Transformation-Induced Plasticity) and TWIP (Twinning-Induced Plasticity), which make them ideal for use in demanding environments where both toughness and elongation are critical.

Composition and Characteristics

- Typically contain **3–12 wt% manganese**.
- Enable:
  - ✓ High strength–ductility synergy
  - ✓ Good crash energy absorption
  - ✓ Advanced phase transformation mechanisms (TRIP/TWIP)
- Targeted for applications requiring **lightweighting with safety**, such as automotive crash zones.

Table 1.1: Mn Steel Comparison

Property	Low Mn Steels	Medium Mn Steels	High Mn Steels
Mn Content	0.5-2%	3-12%	>15-30%
Primary Phases	Ferrite + Pearlite	Ferrite+Retained Austenite(+Martensite)	Austenite-dominanat
Strength&Ductility	Moderate	High	High
TRIP/TWIP	Absent	Present	Mainly TWIP
Applications	General Structures	Automotive (AHSS)	Cryogenics,deep draw

Role of Retained Austenite

- Retained austenite is a metastable FCC phase present at room temperature.
- Under deformation, it:
  - ✓ Transforms to martensite → TRIP effect
  - ✓ Forms twins inside grains → TWIP effect
- These effects:
  - ✓ Enhance strength
  - ✓ Improve ductility
  - ✓ Delay fracture during stress

Table 1.2: Mechanical roles of phases in Medium Mn steel

Phase	Structure	Behavior	Stability
Ferrite	BCC	Soft, ductile	Stable
Retained Austenite	FCC	Transforms or twins under stress	Metastable
Martensite	BCT	Hard, strong	Formed under strain

Challenges and Importance

- Retained austenite is difficult to detect and stabilize due to:
  - ✓ Low volume fraction
  - ✓ Fine dispersion
- Stability influenced by:
  - ✓ Mn, C, and Al content
  - ✓ Heat treatment (quenching, intercritical annealing)
- Effective stabilization enhances formability without sacrificing strength

CHAPTER 2

Literature Review

➢ Evolution from TWIP to Medium Mn Steels

High-Mn TWIP steels (15–30 wt% Mn) once promised outstanding ductility due to their twinning-based deformation. However, several drawbacks emerged with their widespread use: high alloying cost, processing difficulties (due to segregation and solidification issues), and limited weldability. In response, researchers turned to MMnS, where Mn content is significantly lower but TRIP and TWIP effects can still be activated through proper microstructural control.

The ability to stabilize austenite at room temperature with as little as 4–10 wt% Mn, aided by precise thermal treatment, represented a breakthrough. In this class of steels, careful control of Mn and carbon partitioning during intercritical annealing enables the formation of sufficient retained austenite, providing mechanical behavior comparable to high-Mn TWIP steels but at a lower cost and with greater industrial scalability.

➢ Austenite Stabilization: Thermodynamics and Partitioning

The stability of retained austenite is determined by **Mn and C enrichment** during intercritical annealing. These elements lower the martensite start temperature (Ms) and raise the stacking fault energy (SFE), which stabilizes the austenite phase at room temperature.

- **Mn** decreases the Ms and raises SFE up to a point (~10–16 wt%).
- **C** raises SFE significantly and delays martensitic transformation.

Table 1.3: Elements effects on Austenite Stability and SFE

Element	Stabilization	SFE	Additional Rule
Mn	Strong	Parabolic	Segregates atdefects
C	Very Strong	Linear ↑↑	Affects strain aging, stability
Al	Weakens Austenite	↑	Reduces density, forms ferrite
Si	Neutral/Weak	↓	Strengthens ferrite, suppresses cementite

➢ Austenite Formation Kinetics and Interface Dynamics

In addition to thermodynamic considerations, the kinetics of austenite formation play a critical role in determining its fraction and distribution. Intercritical annealing initiates transformation from ferrite (or martensite) to austenite via diffusion-controlled mechanisms. Initially, carbon diffusion dominates, allowing a fast growth of austenite under the NPLE (non-partitioning local equilibrium) regime. As time progresses, Mn partitioning becomes rate-limiting, transitioning the system into the PLE (partitioning local equilibrium) condition, where slower Mn diffusion dictates further austenite growth.

Intercritical annealing initiates transformation through **NPLE and PLE mechanisms**:

- **Stage I (NPLE)**: Fast carbon-controlled growth.
- **Stage II (PLE)**: Slower manganese-diffusion-controlled growth.
- **Stage III**: Stabilization as equilibrium is approached.

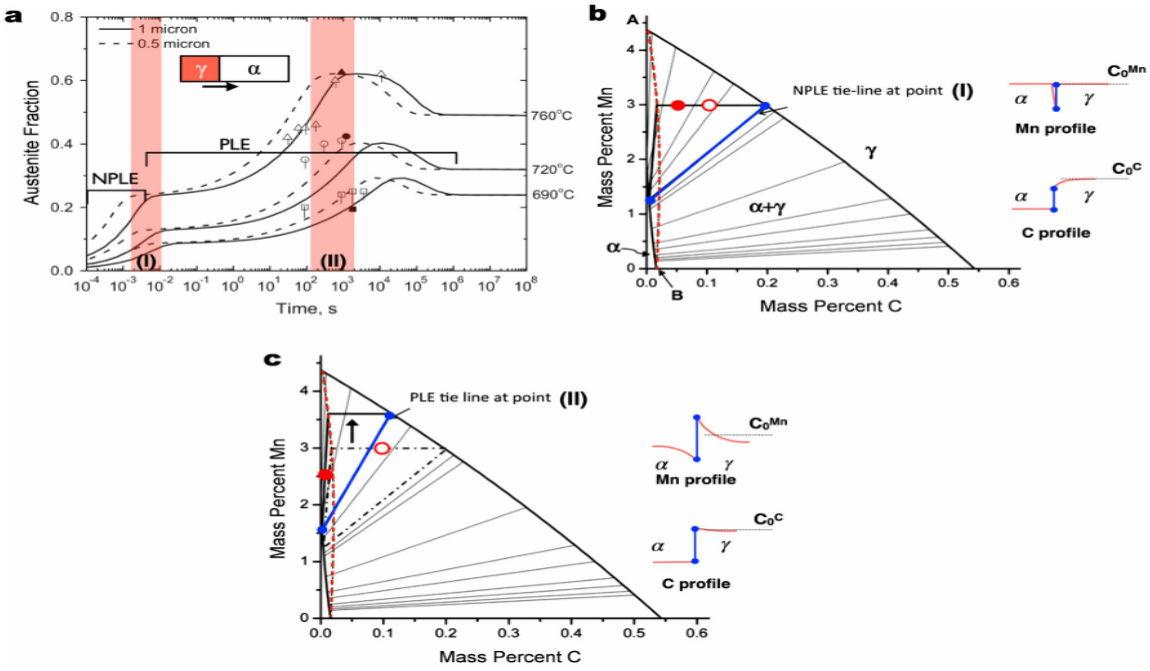

Fig 1.1: Transformation behavior and partitioning during austenite reversion

➢ Role and Morphology of Retained Austenite

Retained austenite in MMnS typically forms in three morphologies:

- **Film-type austenite** located between ferrite grains, characterized by high stability due to constrained geometry.
- **Blocky austenite**, larger in size and less stable, prone to early transformation during deformation.

- **Grain boundary austenite**, nucleating along prior austenite or martensite boundaries.

Film-type austenite is the most desirable for enabling the TRIP effect, as it transforms gradually under strain, supporting work hardening over a prolonged deformation range. In contrast, blocky austenite may transform too early, limiting its contribution to elongation.

The morphology is influenced by thermal processing and the presence of microstructural features such as dislocations, carbides, and solute segregation zones.

➢ Influence of Carbides on Austenite Reversion

Carbides—primarily cementite—affect austenite formation in both positive and negative ways. They serve as nucleation sites during intercritical annealing, especially when reversion occurs from martensite, where residual cementite remains. However, they also act as carbon sinks, potentially depleting surrounding areas of the carbon needed to stabilie austenite.

The presence of Mn-rich cementite, common in medium Mn steels, further complicates the process. Due to Mn's sluggish diffusion, its partitioning from carbides to austenite is extremely slow, often resulting in Mn-deficient and thus unstable austenite. Simulations have shown that austenite reversion is considerably slower in steels containing high levels of residual carbides unless the annealing temperature and duration are carefully optimized.

➢ Solute Segregation and Interfacial Stabilization

Grain boundaries and dislocations act as favorable sites for austenite nucleation due to:

- **Mn segregation**, which lowers local Gibbs energy.
- **Carbon enrichment**, which further enhances stability.

Studies show that **segregated regions can initiate austenite reversion** even below typical equilibrium temperatures, and that the **spinodal-like fluctuations** in composition act as precursors to transformation.

➢ Mechanical Behavior: TRIP Effect and Austenite Stability

The mechanical performance of MMnS depends heavily on the **timing and stability** of the austenite-to-martensite transformation.

- **Stable austenite**: Transforms gradually, enhances ductility and energy absorption.
- **Unstable austenite**: Transforms early, increases strength but may limit elongation.

Table 1.4: Typical Mechanical properties of medium Mn steels with retained austenite

Austenite Volume %	Yield Strength MPa	UTS MPa	Total Elongation %
~10%	850	1050	25
~20%	800	1200	30-35
~30%	700	1300	40+

➢ Experimental and Simulation Approaches

To understand and quantify retained austenite, a range of techniques have been utilized:

- **XRD**: Standard for phase identification but limited for detecting finely dispersed or low-volume austenite.
- **EBSD**: Provides crystallographic information and spatial distribution of phases.
- **APT**: Offers atomic-scale insights into solute partitioning and segregation behavior.
- **Nanoindentation**: Used for mapping mechanical properties of individual phases.
- **DICTRA and Thermo-Calc**: Applied for simulating diffusion-controlled transformations and equilibrium phase diagrams.

While each technique has strengths, their combination is often necessary to obtain a full understanding of phase behavior.

➢ Challenges and Research Directions

Despite extensive work, challenges remain in:

- Accurately quantifying **finely dispersed retained austenite**.
- Understanding **local phase stability** at grain boundaries and interfaces.
- Translating lab-scale findings to **industrial-scale heat treatments**.
- Designing **cost-effective compositions** that balance alloy content, stability, and performance.

Future research should aim to:

- Develop high-resolution, multi-modal characterization pipelines.
- Design optimized intercritical annealing treatments for reproducible austenite stabilization.
- Study deformation-induced transformation under real service conditions.

CHAPTER 3
EXPERIMENT

The chemical composition of the medium manganese steel sample used in this study is:

Table 1.5 Sample Composition

Element	Weight %
Mn	6
C	0.3
Al	3
Si	1.5
Fe	Remaining

➢ Sample Preparation

1. **Sample Mounting**: Hot mounting using thermosetting resin for better handling and edge retention.
2. **Leveling**: Bubble leveler attached during mounting to ensure flatness of the surface.
3. **Grinding**: Used SiC abrasive papers (240 to 1200 grit) to remove surface damage.
4. **Polishing**: Cloth polishing with Silica to achieve a mirror-like surface finish.
5. **Ultrasonic Cleaning**: Cleaned in distilled water and ethanol solution to remove fine debris.
6. **Etching**: Etched with 0.2% Nital to reveal microstructure.

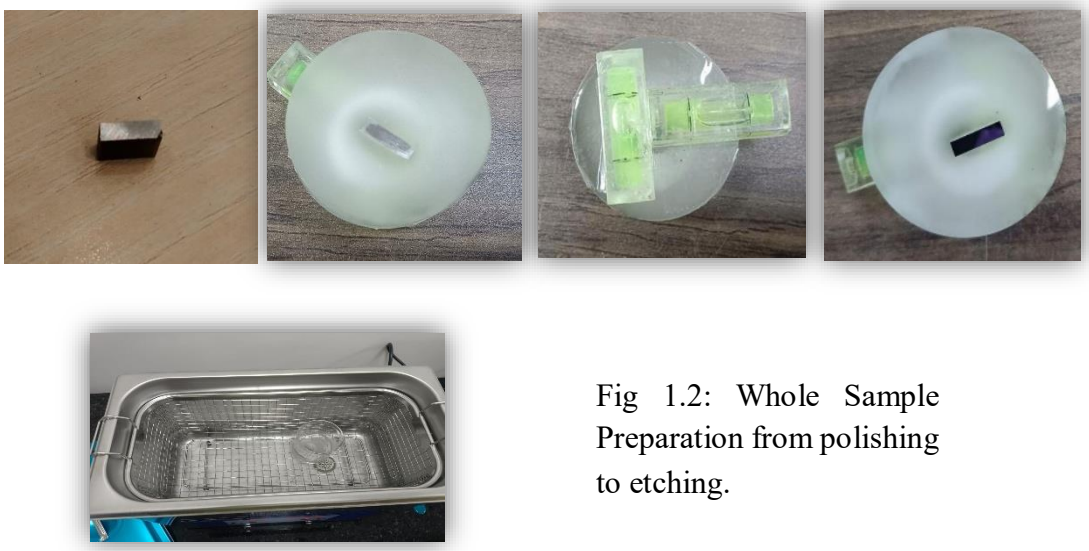

Fig 1.2: Whole Sample Preparation from polishing to etching.

OPTICAL MICROSCOPY
METHODOLOGY

1. **Microscopy Setup**

- The sample was examined using a bright-field optical microscope.
- Multiple images were captured and stitched together to get a larger view of the microstructure.

2. **Etching for Contrast**

- Etching was done using 0.2% Nital solution to differentiate phases.
- Brighter regions indicated ferrite, while darker regions represented retained austenite or martensite.

3. **Phase Identification**

- The contrast from etching helped visually distinguish between ferrite and austenite.
- Ferrite appeared light due to its faster etching rate, and austenite appeared dark as it etched slower.

4. **Image Analysis**

- ImageJ software was used to analyze the micrographs.
- To calculate phase fractions by line intercept method for light and dark regions and also Grain size measurement.

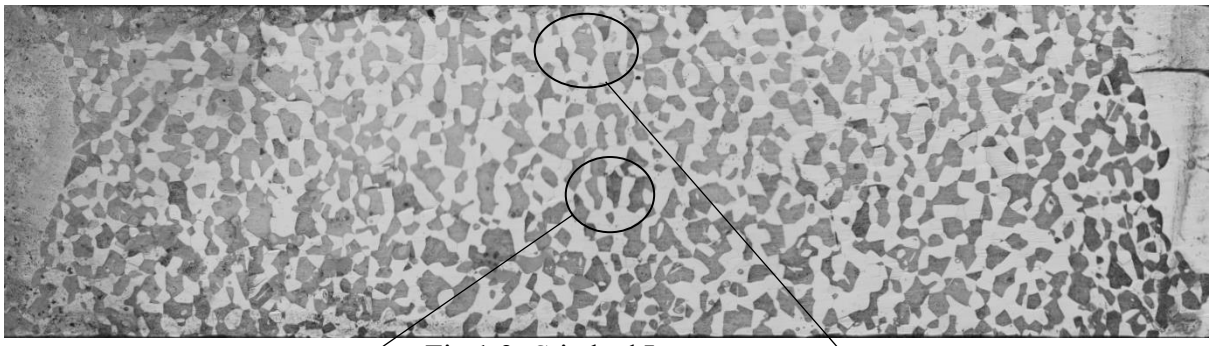

Fig 1.3: Stitched Image

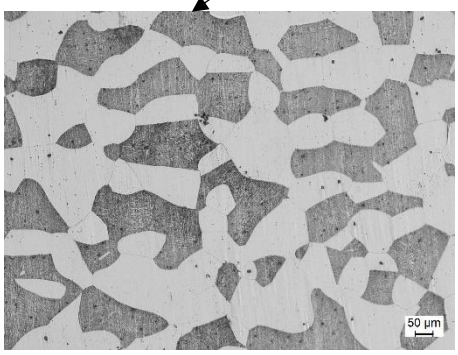

Fig 1.4a: Microstructure at 100x

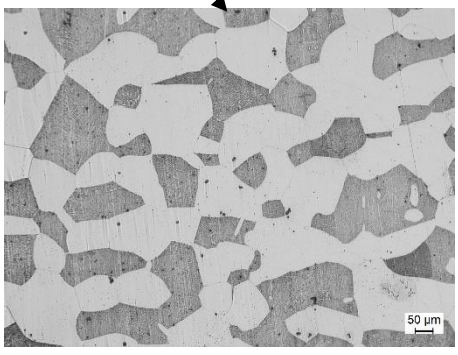

Fig 1.4b: Microstructure at 100x

Phase Fraction and Grain Size Measurement

1. Phase Fraction Calculation

- The phase fraction was calculated using the line intercept method on optical micrographs.
- Multiple straight lines were drawn across different areas of the stitched image.
- Intersections with Bright and dark regions were counted.
- From these counts, the phase fractions were determined as:
  - Brighter phase: 54.6%
  - Darker phase: 45.4%

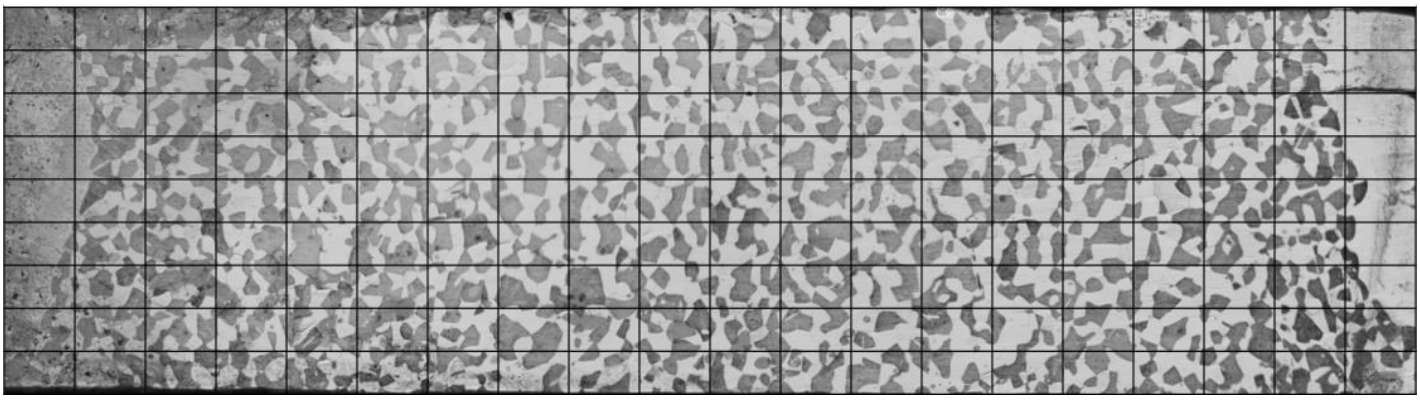

Fig 1.5: Phase Fraction Calculation using line intercept method

2. Grain Size Measurement

- Grain size was also measured using the line intercept method.
- Average grain size was taken.
- Results showed:
  - Brighter grains: Primarily in the 125–150 µm range (coarser).
  - Darker grains: Around 150–200 µm, appearing more uniformly distributed but finer in texture.

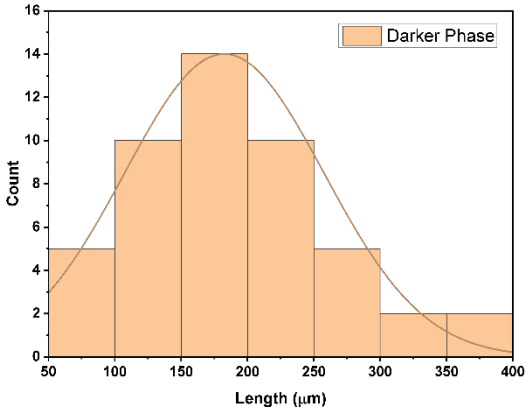

Fig 1.6a: Grain Size range of Darker Phase

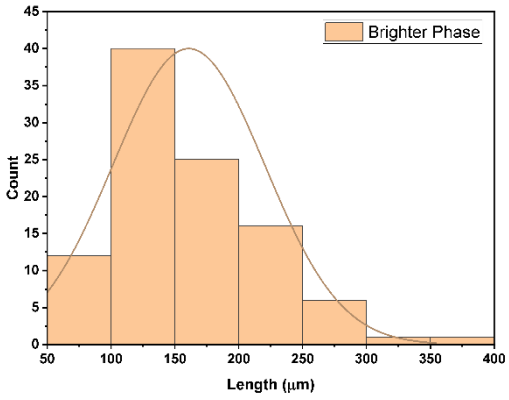

Fig 1.6b: Grain Size range of Brighter Phase

3. **Multiple Area Averaging**
    - Calculations were performed across several regions to reduce local variation and improve statistical reliability.

➢ Results And Observations

1. **Ferrite (Brighter Regions – 54.6%)**
    - Ferrite forms the **majority phase**, comprising 54.6% of the microstructure.
    - Its **coarser grain size** (125–150 µm) suggests it underwent more grain growth during processing, possibly due to higher thermal stability.
    - The larger grain size of ferrite contributes to **good ductility and formability**, as dislocation motion is less restricted.
    - Its bright appearance under the microscope is due to **higher etching response** and surface roughening from its BCC structure.

2. **Retained Austenite (Darker Regions – 45.4%)**
    - Retained austenite makes up 45.4% of the structure, indicating successful stabilization through Mn and C additions.
    - It exhibits a **finer grain size** (150–200 µm range) and appears more uniformly distributed across the matrix.
    - The smaller grain size improves **mechanical stability**, helping austenite resist premature transformation and enabling the **TRIP effect** during deformation.
    - The darker appearance is due to its **lower etching rate**, typical of FCC structures, and smoother etched surface.

3. **Microstructural Balance and Performance**
    - The near-equal distribution of ferrite and austenite phases supports an optimal balance between **strength and ductility**.
    - Coarse ferrite ensures ductility, while fine, retained austenite offers potential for transformation-induced plasticity, improving **strain hardening and toughness**.
    - This dual-phase structure is ideal for applications requiring **lightweight, high-strength steels** with good formability.

X-RAY DIFFRACTION

METHODOLOGY

1. **Instrument Setup**
   - XRD analysis was performed using a Cu-Kα source (λ ≈ 1.54 Å).
   - Scanning was done over a wide 2θ range to capture all major peaks.
   - We have done 2 scans for perfection.

2. **Data Collection**
   - The sample surface was prepared via standard polishing and etched only lightly to preserve crystallographic integrity.
   - XRD patterns were recorded and exported for further analysis.

3. **Phase Identification**
   - Peak positions were analyzed to determine d-spacings and calculate crystal structure using Bragg's Law.
   - A list of peak 2θ values, corresponding θ, and calculated sin2θ values were used to identify lattice type based on their ratio.

➢ Results & Graphs

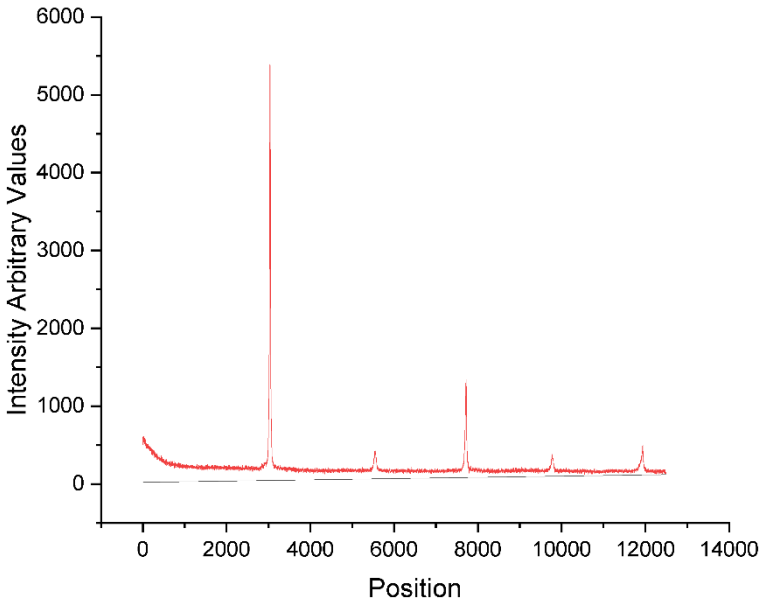

Fig 1.7a: XRD Peaks for Scan 1

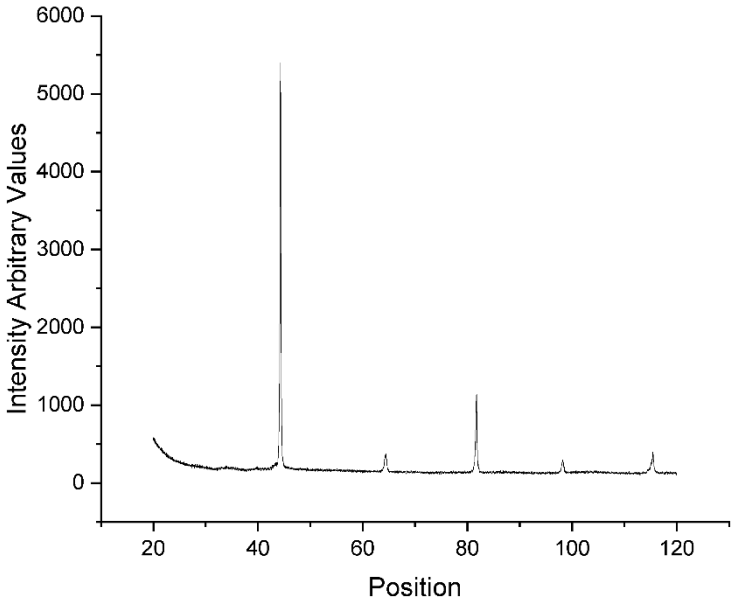

Fig 1.7b: XRD Peaks for Scan 2

➢ Calculations

Pos.[2Th.]	d spacing	Theta	Sin(theta)	Sin^2(theta)	Ratio
44.307	2.0427	22.15	0.377	0.1421	1
64.393	1.4457	32.19	0.5328	0.2838	2
81.735	1.1772	40.86	0.6543	0.4281	3
98.225	1.0189	49.11	0.7559	0.5713	4
115.44	0.9111	57.72	0.8454	0.7147	5

Table 1.6: Calculation of XRD peaks in Scan 1

Pos.[2Th.]	d spacing	Theta	Sin(theta)	Sin^2(theta)	Ratio
44.308	2.04271	22.15	0.377	0.1421	1
64.391	1.44573	32.19	0.5328	0.2838	2
81.73	1.17732	40.86	0.65427	0.42806	3
98.229	1.01889	49.11	0.756	0.5715	4
115.421	0.91121	57.71	0.84535	0.71461	5

Table 1.7: Calculation of XRD peaks in Scan 2

1. **Using Bragg's Law: $n\lambda=2d\sin\theta$**
    - Where d is the interplanar spacing, θ is half the 2θ peak position, and λ is the wavelength.

2. **Determining Lattice Type:**
    - $\sin^2\theta$ values were normalized to the smallest value.
    - The resulting ratio **(1:2:3:4:5)** matches that of BCC structures, confirming the dominant phase as ferrite.

3. **Peak Analysis Summary:**
    - Consistent spacing and peak intensity match BCC ferrite.
    - No significant peaks corresponding to FCC (austenite) were observed, suggesting it is either absent, transformed to martensite, or present in quantities below XRD detection limits.

➢ Observations

1. The XRD results indicate that the **dominant crystalline structure is BCC**, which corresponds to the **ferrite phase**.
2. The **retained austenite phase was not clearly detected** in the XRD pattern. This may be due to:
    - Its low volume fraction in the sample.
    - Fine dispersion or nanocrystalline form, making it difficult to detect.
    - Possible transformation into **martensite** during cooling after heat treatment.
3. The data supports optical microscopy findings where ferrite was the **major phase (54.6%)**, appearing as bright regions.
4. XRD, while excellent for identifying dominant crystal structures, may **underestimate retained austenite** when present in fine or low concentrations — suggesting the need for more sensitive techniques like EBSD or synchrotron XRD in future work.

SEM – EDX ANALYSIS

METHODOLOGY

1. **Sample Preparation**
    - The same polished and etched sample used for optical microscopy was analyzed under SEM.
    - Conductive carbon coating was applied to prevent surface charging during imaging.

2. **SEM Imaging Parameters**
    - SEM was conducted at an accelerating voltage of 20 kV.
    - Multiple regions were imaged to assess surface morphology and phase distribution.

3. **EDX (Energy Dispersive X-ray) Analysis**
    - EDX spectra were acquired from two distinct contrast regions:
        - Brighter phase
        - Darker phase
    - Acquisition time: 45 minutes for accurate elemental quantification.

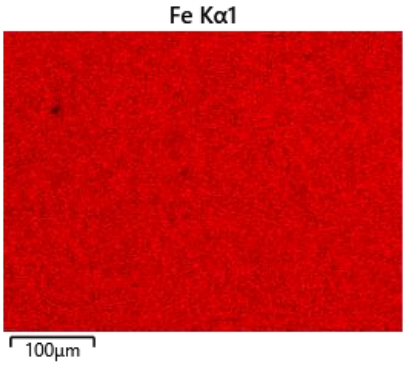

Fig 1.8a: EDX Fe Mapping

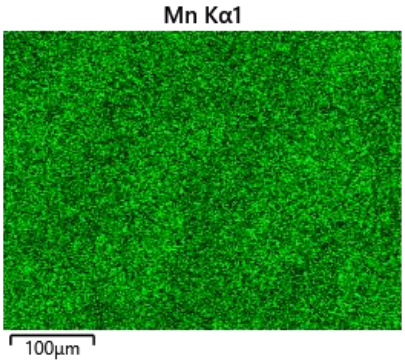

Fig 1.8b: EDX Mn Mapping

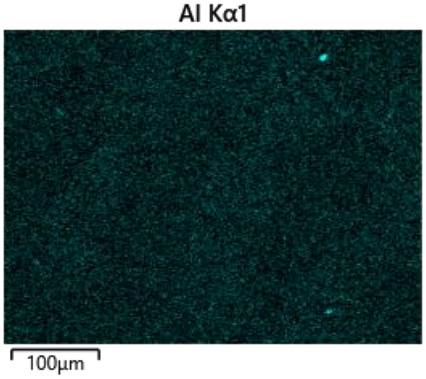

Fig 1.8c: EDX Al Mapping

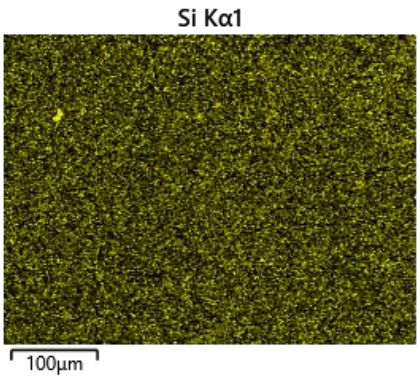

Fig 1.8d: EDX Si Mapping

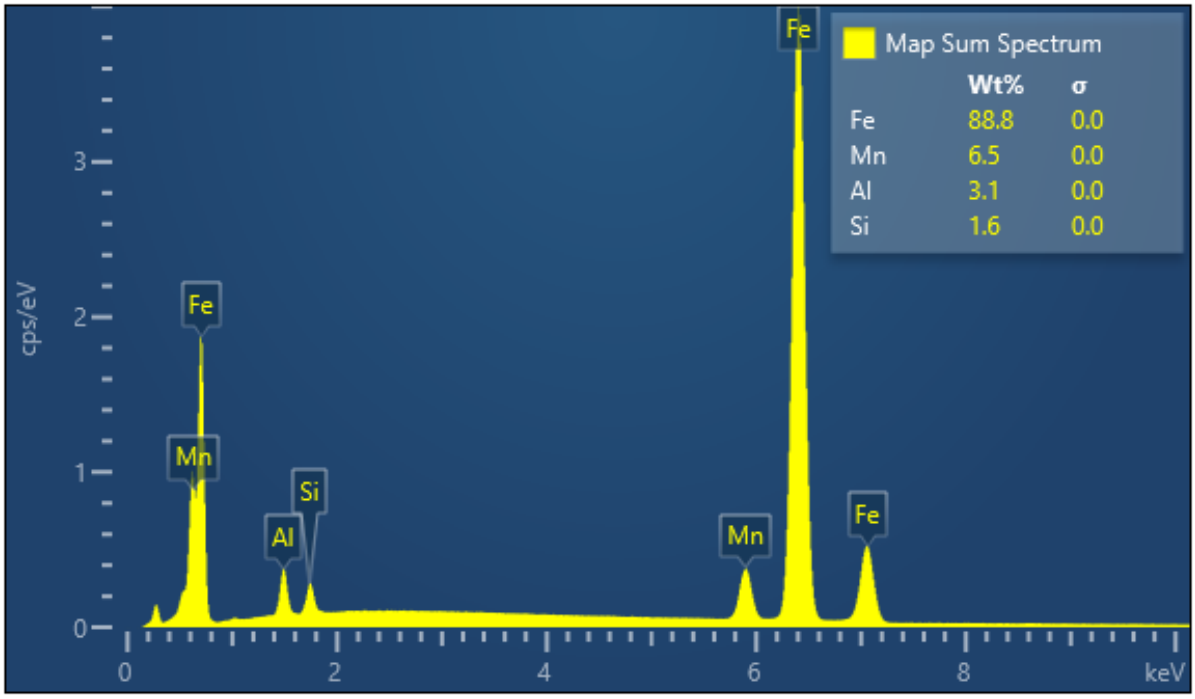

Fig 2.1: ALL Elements Map Spectrum

➢ Results

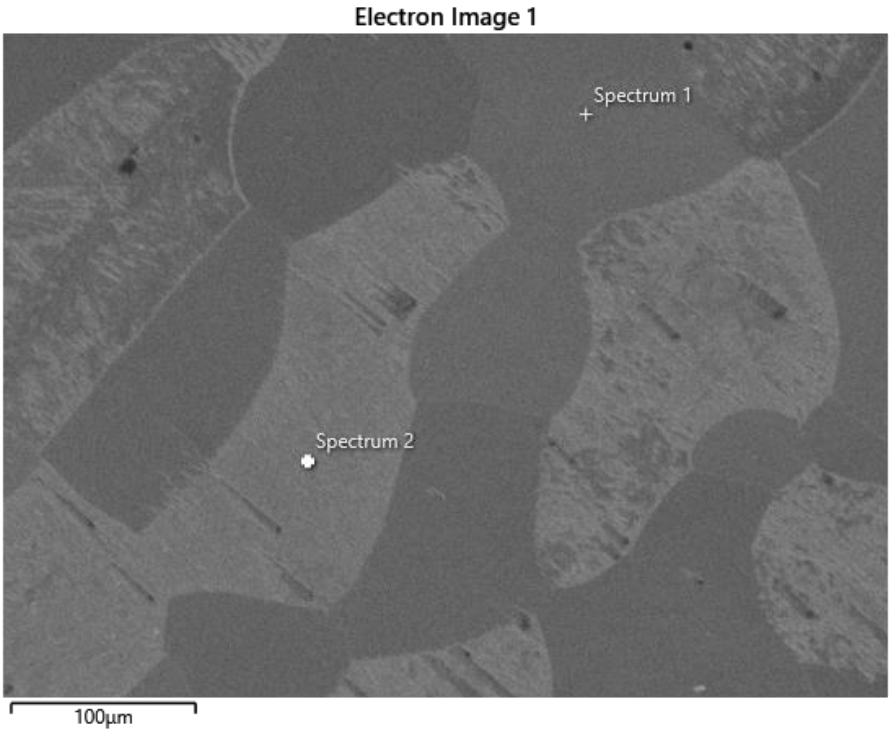

Fig 2.2: SEM Image

✓ **Spectrum 1 (Darker Phase – Likely Ferrite)**

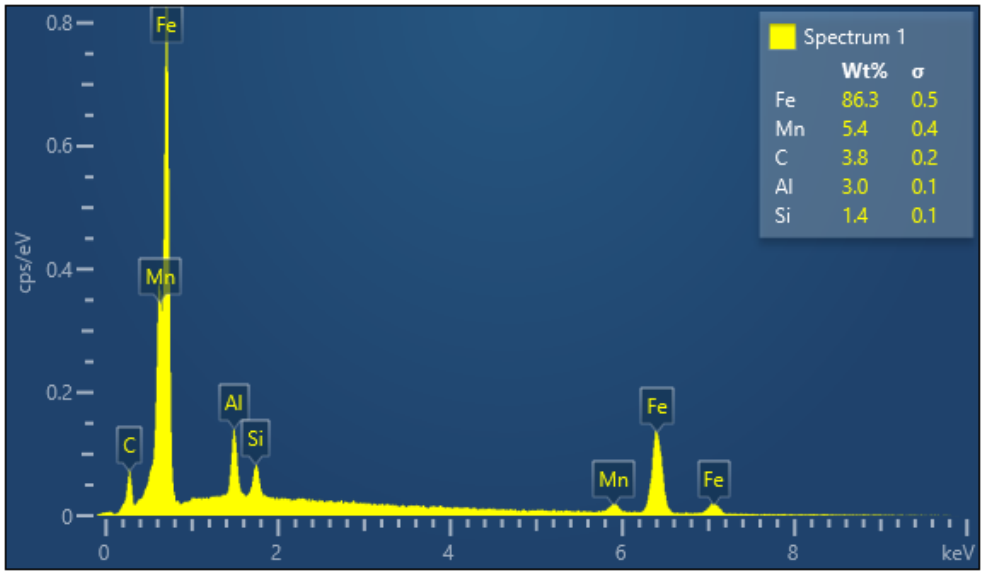

Fig 2.3: Spectrum 1 elemental mapping

Table 1.8: Elemental Composition in Spectrum 1

Element	Weight %
Fe	86.3
Mn	5.4
C	3.8
Al	3.0
Si	1.4

- Higher Fe and Al content with lower Mn.
- Indicates this region is ferrite, since Al stabilizes ferrite and its presence is higher here.

✓ **Spectrum 2 (Brighter Phase – Likely Retained Austenite)**

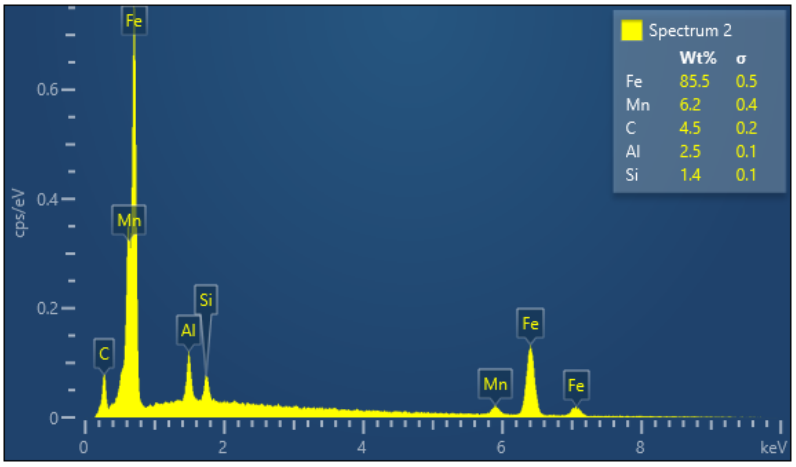

Fig 2.4: Spectrum 2 elemental mapping

Table 1.9: Elemental Composition in Spectrum 2

Element	Weight %
Fe	85.5
Mn	6.2
C	4.5
Al	2.5
Si	1.4

- Higher Mn and slightly higher C, with less Al compared to Spectrum 1.
- Suggests this region is retained austenite, as Mn stabilizes austenite (FCC structure).

➢ Observations

1. **Phase Identification by Chemistry**
    - **Darker Region (Spectrum 1):**
        - More Al → ferrite stabilizer
        - Less Mn → consistent with BCC ferrite
        - Concludes: **Ferrite phase**
    - **Brighter Region (Spectrum 2):**
        - Higher Mn → stabilizes retained austenite
        - Higher C also aids austenite retention
        - Concludes: **Retained austenite phase**
2. **Carbon Content Analysis**
    - Carbon appears higher in both regions (3.8%–4.5%), which is **above expected values**.
    - This is likely due to:
        - **Overestimation by EDX** (common for light elements)
        - **Surface contamination** (e.g., carbon tape, mounting resin, polishing residues)
        - **Interaction depth**, where the beam may pick up carbon from below the surface.
3. **Phase Support from Element Trends**
    - **Mn ↑ & Al ↓ → Austenite**
    - **Mn ↓ & Al ↑ → Ferrite**
    - This elemental partitioning reinforces the dual-phase microstructure observed in optical microscopy and XRD.
4. **Microstructural Implication**
    - The presence of both phases confirms the alloy's design intent for **TRIP behavior**, where retained austenite contributes to deformation hardening and ferrite provides ductility.

NANO INDENTATION

METHODOLOGY

1. **Equipment and Indenter**
   - Nanoindentation tests were carried out using a Berkovich diamond tip indenter.
   - The machine recorded **load-displacement curves** to extract mechanical properties at microscale.

2. **Test Parameters**
   - Multiple indentations were made in both **brighter and darker regions** (from optical/SEM contrast) to separately characterize **ferrite**, **martensite**, and **retained austenite**.
   - The Poisson's ratio for the sample was assumed to be **vs = 0.34**, and for the diamond indenter **vi = 0.07**, with **Ei = 1140 GPa**.

3. **Data Analysis**
   - The **reduced elastic modulus (Er)** was calculated from unloading curves.
   - The actual **elastic modulus (E)** of the sample was derived using the following relation:

$$\frac{1}{E_r} = \frac{1-\nu_s^2}{E_s} + \frac{1-\nu_i^2}{E_i}$$

➢ Results

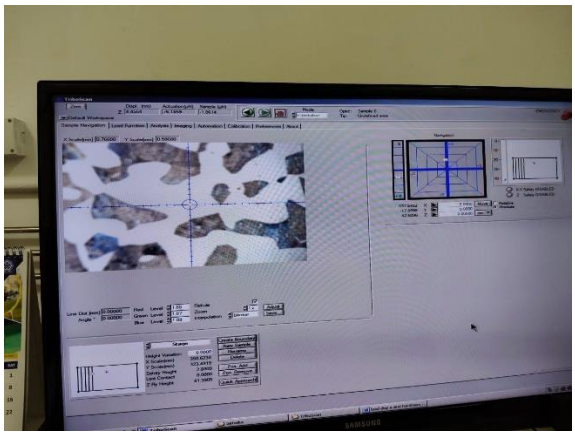

Fig 2.5a: Nano Indentation test interface Brighter Area

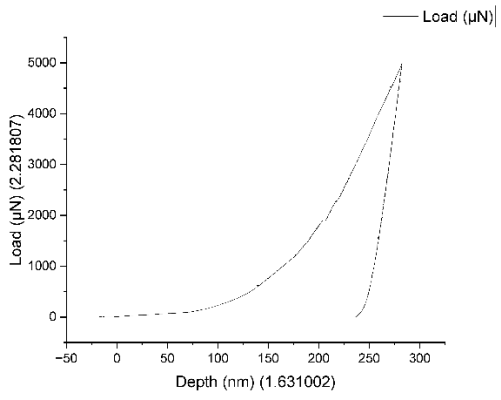

Fig 2.5b: Load Vs Depth Curve

Brighter Area - Ferrite
Er = 135GPa
H = 4GPa
E = 135.324386GPa

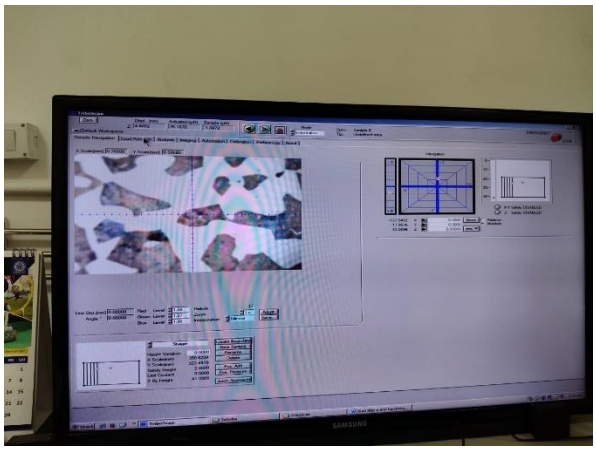

Fig 2.6a: Nano Indentation test interface Darker Area 1

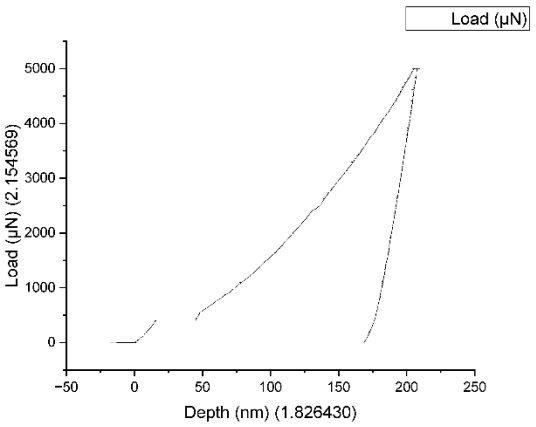

Fig 2.6b: Load Vs Depth curve Darker Area 1

Darker Area - Ferrite
Er = 111GPa
H = 4.8GPa
E = 108.688GPa

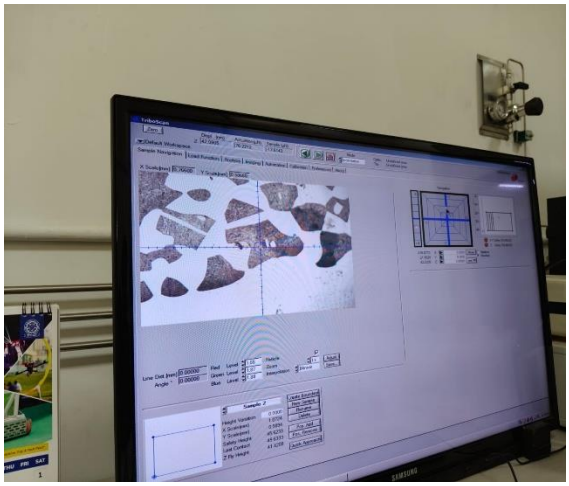

Fig 2.7a: Nano Indentation test interface Darker Area 2

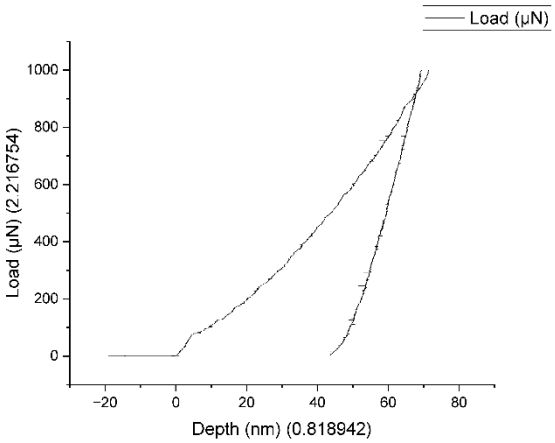

Fig 2.7b: Load Vs Depth curve Darker Area 2

Darker Area - Martensite
Er = 99.40GPa
H = 5.87GPa
E = 96.2521GPa

Table 2.1: Nano Indentation results

Region	E_r (GPa)	Hardness (GPa)	Elastic Modulus (GPa)
Brighter (Ferrite)	135	4.0	135.3
Darker (Martensite)	99.4	5.87	96.3
Darker (Austenite)	111	4.8	108.7

- **Ferrite** showed relatively low hardness and high elastic modulus, consistent with a soft, ductile phase.
- **Martensite** displayed the highest hardness, indicating its strong and brittle nature.

➢ Observations

1. **Ferrite (Brighter Area):**
    - Exhibited **lower hardness (~4 GPa)** but a **higher elastic modulus (~135 GPa)**.
    - Indicates ductile behavior with efficient load distribution and deformation.
2. **Martensite (Darker Area):**
    - Recorded **highest hardness (~5.87 GPa)** with **lower modulus (~96 GPa)**.
    - Suggests a **hard but less stiff phase**, likely due to high dislocation density and strain from phase transformation.
3. **Retained Austenite / Mixed Regions:**
    - Intermediate values were seen in some darker regions, indicating possible **retained austenite or partial transformation to martensite**.
4. **Elastic Modulus Consistency:**
    - Despite hardness differences, the elastic modulus values for all phases remained in a narrow range (96–135 GPa), as **modulus is governed more by atomic bonding than microstructure**.
5. **Microstructural Implication:**
    - The nanoindentation results support the **phase-specific mechanical behavior** observed in dual-phase steels:
        - **Ferrite → Soft, ductile matrix**
        - **Martensite → Hard, strengthening phase**
        - **Retained Austenite → Can transform under stress (TRIP), contributing to strength and ductility**

CHAPTER 4
Proposed Work

Objectives

- Optimize retained austenite fraction through thermal/mechanical treatment.
- Study the effect of deformation on austenite stability.
- Perform advanced characterization using EBSD and/or synchrotron XRD.
- Correlate microstructure with mechanical behavior (tensile, nanoindentation).

Description of Work

- **Objective 1: Austenite Optimization**
  Design and perform heat treatments (intercritical annealing, quenching) to vary austenite content.

- **Objective 2: Stability under Deformation**
  Apply controlled deformation (tensile tests), observe retained austenite transformation using XRD/EBSD.

- **Objective 3: Advanced Characterization**
  Use Electron Backscatter Diffraction (EBSD) to map phase and orientation; synchrotron XRD for low-volume austenite detection.

- **Objective 4: Property Correlation**
  Analyze tensile/nanoindentation results and correlate with phase distribution and transformation behavior.

➢ **Flow Chart of Proposed Work**

Sample Selection

↓

Heat Treatment Optimization

↓

Mechanical Deformation

↓

Advanced Characterization (EBSD, XRD)

↓

Data Analysis & Phase Quantification

↓

Property–Microstructure Correlation

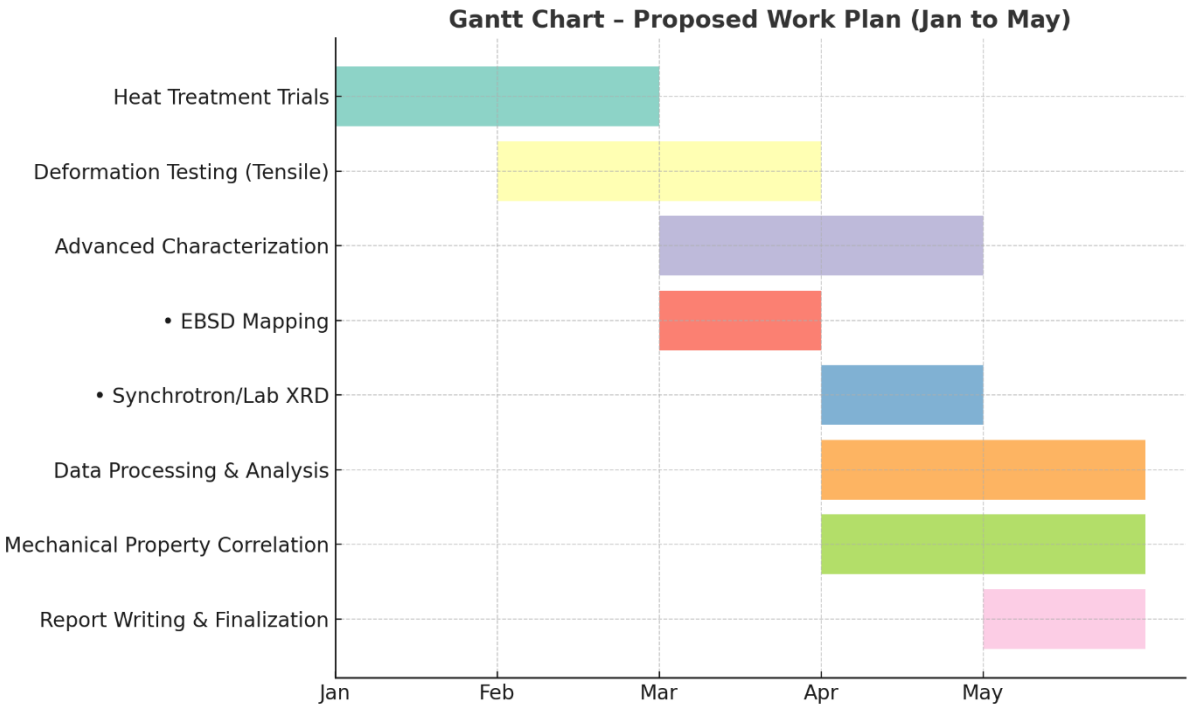

Fig 2.8: Gantt Chart for Proposed Work Plan for next semester

CHAPTER 5

Summary

This report investigates the role of **retained austenite** in a **medium manganese steel** composition (Fe–6Mn–0.3C–3Al–1.5Si) aimed at achieving a balance of **high strength and ductility**. The focus is on understanding the contribution of retained austenite to mechanical behavior through the **TRIP effect (Transformation-Induced Plasticity)**.

A series of characterization techniques were used:

- **Optical Microscopy** confirmed a dual-phase structure with ~54.6% ferrite and ~45.4% retained austenite.
- **XRD** identified the dominant phase as BCC ferrite; retained austenite was not detected due to its fine dispersion or low volume.
- **SEM-EDX** revealed phase-specific chemistry: higher Mn in brighter regions (austenite) and higher Al in darker regions (ferrite).
- **Nanoindentation** showed ferrite had lower hardness but higher modulus, while martensite had higher hardness, indicating phase-specific mechanical roles.

✓ **Automotive Application Relevance**

Medium Mn steels with retained austenite are ideal for **third-generation AHSS** used in automotive structures. The **TRIP effect** improves strength during deformation, while the ferrite matrix provides ductility and formability. This allows for **lightweight design**, improved **crash energy absorption**, and better **fuel efficiency**, making such steels highly suitable for safety-critical and structural components in modern vehicles.

CHAPTER 6
References

[1] D.V. Edmonds, K. He, F.C. Rizzo, B.C. De Cooman, D.K. Matlock, J.G. Speer, *Mater. Sci. Eng. A* **2006**, *438–440*, 25–34.

[2] J.G. Speer, D.K. Matlock, B.C. De Cooman, J.G. Schroth, *Acta Mater.* **2003**, *51*, 2611–2622.

[3] B.C. De Cooman, K.G. Chin, J. Kim, *Acta Mater.* **2012**, *60*, 583–598.

[4] C. Scott, S. Allain, N. Gey, M. Humbert, *Mater. Sci. Eng. A* **2006**, *429*, 352–360.

[5] H. Ding, L. Guo, Z. Xie, Y. Deng, L. Cheng, *Mater. Sci. Eng. A* **2020**, *776*, 139035.

[6] L. Qian, X. Wu, L. Wang, *J. Mater. Sci. Technol.* **2020**, *43*, 176–185.

[7] Y. Shen, R. Zhi, H. Yang, Z. Sun, *Mater. Charact.* **2016**, *118*, 469–475.

[8] X. Wang, Y. Wang, J. Li, C. Wang, *J. Alloys Compd.* **2019**, *775*, 961–969.

[9] G. Krauss, *Steels: Processing, Structure, and Performance*, 2nd ed., ASM International, 2015.